RASĀYAN *J. Chem.*
Vol. 19 | No. 3 | 1396-1403 | July-September | 2026
ISSN: 0974-1496 | e-ISSN: 0976-0083 | CODEN: RJCABP
http://www.rasayanjournal.com
http://www.rasayanjournal.co.in

UPLC-HRMS/MS-BASED CHEMOPROFILING AND BIOACTIVITY EVALUATION OF PHLOGACANTHUS CORNUTUS EXTRACT

T. T. Nha Tran[1,✉] and T. P. Nhung Tran[2]
[1]Faculty of Chemical Engineering, Industrial University of Ho Chi Minh City, 700000, Vietnam
[2]Institute of Biotechnology - Food, Industrial University of Ho Chi Minh City, 700000, Vietnam
✉Corresponding author: tranthithanhnha@iuh.edu.vn

ABSTRACT

Untargeted LC-HRMS/MS metabolomics has become a key approach for characterizing the complex chemical composition of plant extracts; however, integrating multiple annotation platforms into a coherent chemoprofiling framework remains challenging. In this study, an integrated workflow combining MZmine, MS-DIAL, GNPS feature-based molecular networking, and SIRIUS was applied to systematically annotate metabolites in *Phlogacanthus cornutus*, a recently described species with limited phytochemical information. Integrated analysis of positive and negative UPLC-MS/MS revealed that the metabolite profile of *Phlogacanthus cornutus* is dominated by iridoid glycosides (including harpagoside and harpagide), hydroxylated diterpenoids, oxylipins, monoacylglycerols, and minor phenolic constituents. Merging polarity-specific ion forms improved annotation coherence and reduced redundancy relative to single-mode analysis. Bioactivity assays demonstrated concentration-dependent nitric oxide inhibition (IC50 = 19.27 ± 1.76 µg/mL) without detectable cytotoxicity, together with measurable antioxidant activity in $ABTS^{\cdot+}$(maximum of 230 mg Trolox/g extract) and FRAP (≈11.2-15.3 mg Fe^{2+}/g extract at 150 ppm) assays. These findings provide the first LC-MS/MS-based chemoprofile of *Phlogacanthus cornutus* and demonstrate the utility of integrating complementary annotation platforms for bioactivity-oriented metabolomics studies. Beyond establishing a phytochemical and bioactivity reference for this understudied species, the proposed workflow may support future natural product discovery, comparative chemotaxonomic studies, and systematic prioritization of bioactive metabolites in medicinal plant research.

Keywords: UPLC-HRMS/MS, *Phlogacanthus cornutus*, metabolites, NO inhibition, $ABTS^{\cdot+}$ scavenging and FRAP
RASĀYAN *J. Chem.*, Vol. 19, No.3, 2026

INTRODUCTION

Recent advances in computational metabolomics have led to the development of integrative workflows that combine data preprocessing, spectral similarity analysis, and in silico structure prediction for large-scale annotation of LC-MS/MS data. Among the most widely adopted tools are MZmine, MS-DIAL, Global Natural Products Social Molecular Networking (GNPS), and SIRIUS, which together form a complementary ecosystem for LC-MS/MS-based phytochemical analysis.[1-5] These platforms enable feature detection, spectral comparison, molecular networking, and computational structure prediction, thereby facilitating metabolite annotation in complex plant extracts even when reference spectra are limited. Recent studies have further emphasised the importance of integrated computational metabolomics workflows for systematic natural product discovery and bioactivity-oriented phytochemical research.[6, 7] This study aligns with Sustainable Development Goal 3 (Good Health and Well-being) through the investigation of bioactive metabolites with potential antioxidant and anti-inflammatory relevance. Among species of the genus *Phlogacanthus, Phlogacanthus cornutus* (Acanthaceae) is a recently described species for which phytochemical information is currently limited to preliminary GC-MS-based profiling, with no comprehensive LC-MS/MS-based and MS/MS-resolved metabolomic characterization reported todate.[8-14] Consequently, the detailed metabolite composition of this species and its potential relationship with biological activities remain largely unexplored. In this study, an integrated UPLC-HRMS/MS analytical framework was applied to investigate the chemical composition and biological activities of *P. cornutus* extract. UPLC-HRMS/MS data were processed using a combined MZmine-MS-DIAL-GNPS-SIRIUS workflow to enable systematic annotation of HRMS/MS features and in silico prediction of

http://doi.org/10.31788/RJC.2026.1939825

candidate molecular structures. The resulting metabolite annotations were further correlated with antioxidant and anti-inflammatory activities to provide an integrated chemoprofiling and bioactivity evaluation of the species. The combined workflow also allowed complementary interpretation of LC-MS/MS data from different ionisation modes, reducing annotation redundancy and improving overall metabolite coverage.

EXPERIMENITAL

Materials

Trolox, reduced L-glutathione, ABTS, TPTZ, and lipopolysaccharides (LPS) from Escherichia coli. N-(1-naphthyl)ethylenediamine dihydrochloride was obtained from Sigma-Aldrich (St. Louis, MO, USA). Cell-based experiments were carried out using Dulbecco's Modified Eagle's Medium (DMEM) supplemented with fetal bovine serum (FBS). Unless otherwise specified, all chemicals and reagents were of analytical grade. Spectrophotometric evaluation of antioxidant capacity was performed on a Thermo Scientific Genesys 20 instrument by monitoring UV–Vis absorbance, whereas nitrite concentrations were measured using a BioTek ELx800 microplate reader.

General Procedure

The overall workflow of this study is illustrated in Fig.-1A, beginning with plant extraction, followed by UPLC-HRMS/MS analysis, feature annotation, compound class evaluation, and subsequent evaluation of nitric oxide inhibition and antioxidant activities.

Plant Extraction

Fresh leaves of *P. cornutus* (Fig.-1B and C) were dried in an oven at 50 °C and subsequently pulverised into a fine powder. A 100 g portion of the dried material was subjected to maceration in 70% (v/v) ethanol at ambient temperature for 72 h. The residue was then extracted twice more using fresh solvent. The pooled extracts were filtered and evaporated under reduced pressure at 50 °C to yield a crude ethanolic extract, which was used for subsequent chemical characterization and bioactivity evaluation.

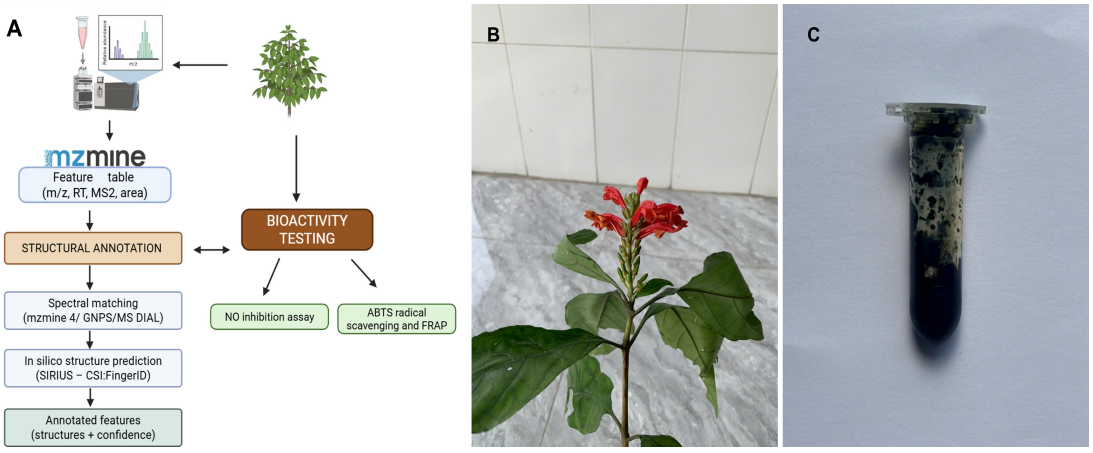

Fig.-1: A. Overview of the Study Workflow: Plant Extraction, UPLC-HRMS/MS Analysis, Metabolite Annotation, And Bioactivity Evaluation. B. The Fresh Leaves and C. The Crude Ethanol Extract of *P. cornutus*

UPLC-HRMS/MS Analysis

The extract was analyzed by UPLC-HRMS/MS in both positive and negative electrospray ionisation modes. UPLC-HRMS/MS analyses were performed using an Exion LC™ system coupled to an X500 R QTOF (SCIEX, USA). Chromatographic separation was achieved on a Hypersil GOLD column. The gradient was programmed as follows: 0-1 min, 98% A; 1-20 min, linear gradient to 98% B; 20-25 min, held at 98% B. Raw data were converted to mzML with ProteoWizard and processed in MZmine for feature detection, alignment, and peak integration. MS/MS spectra were further analyzed using GNPS FBMN, MS-DIAL spectral matching, and SIRIUS (ZODIAC, CSI: FingerID, and CANOPUS) for molecular formula prediction and structural annotation.

Bioactivity Assays

Nitric Oxide (NO) Inhibition

The Griess assay was performed to evaluate nitric oxide (NO) levels in LPS-induced RAW 264.7 macrophages, with absorbance recorded at 540 nm; dexamethasone served as the positive control[15, 16], with cell viability assessed by the MTT method.[17]

Antioxidant Activity

Antioxidant activities of the extract were determined using $ABTS^{\cdot+}$ radical scavenging[18, 19] and ferric reducing antioxidant power (FRAP)[20] assays based on spectrophotometric measurements at 734 nm and 593 nm, respectively. All antioxidant experiments were performed in triplicate.

RESULTS AND DISCUSSION

LC-HRMS/MS-Based Metabolite Annotation of the *P. cornutus* Extract

The base peak chromatograms of *P. cornutus* recorded in negative and positive ionization modes (Fig.-2A and B) revealed a chemically complex extract, with a significant number of metabolites eluting between 4.5 and 20 min. Ion feature annotations obtained in negative mode are summarized in Table-1. The most confidently annotated metabolite cluster corresponded to harpagoside, an iridoid glycoside widely reported in *Pedicularis* species.[21] Harpagoside was detected as the deprotonated ion $[M-H]^-$ at *m/z* 493.1670 and as the formate adduct $[M+HCOO]^-$ at *m/z* 539.1741 (RT 8.60 min) and 539.1721 (RT 8.93 min). In positive ion mode, the corresponding sodiated ions $[M+Na]^+$ were detected at *m/z* 517.1664 and 517.1674 at the same retention times as the two formate counter ions. These ion species were connected through ion identity molecular networking (IIMN) relationships and exhibited consistent retention times and chromatographic peak shapes (Fig.-3A). The MS/MS spectrum of the $[M+HCOO]^-$ ion at *m/z* 539.1741 displayed characteristic fragment ions corresponding to glycosidic bond cleavage and formation of the cinnamate moiety (Fig.-3B).

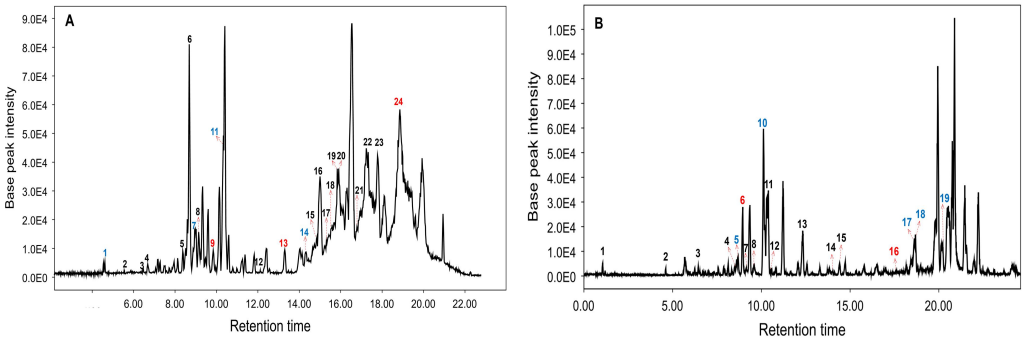

Fig.-2: A. Negative Ion Mode and B. Positive Ion Mode Base Peak Chromatogram (BPC) of *P. cornutus*

The chromatograms illustrate the distribution of annotated LC-MS/MS features across retention time and ionization modes, while annotation details are summarized separately in Table-1.

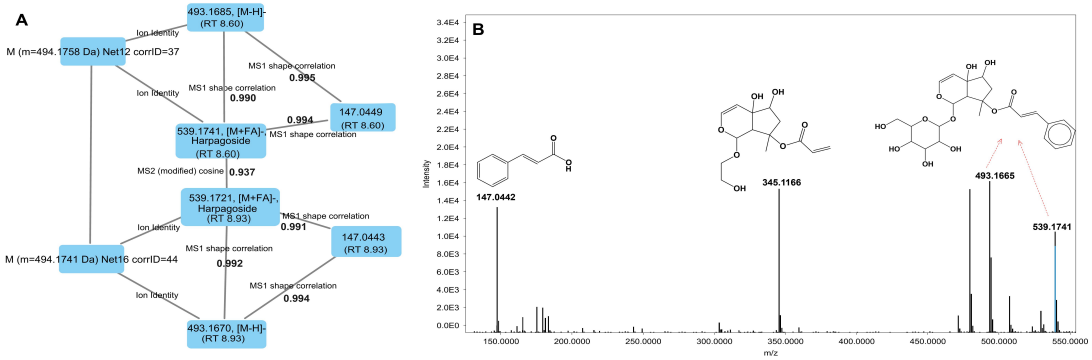

Fig.-3: A. Ion Identity Molecular Networking (IIMN) of the Harpagoside Cluster. B. Negative ESI-CID MS/MS Spectrum of the Precursor Ion at *m/z* 539.1741 ($[M+HCOO]^-$)

Table-1: Putative Annotation of Metabolite Features Detected in Negative Electrospray Ionization (ESI^-) Mode using Three Complementary Platforms (MS-DIAL, MZmine, and GNPS). *x* Indicates no Match Obtained

Peak No.	RT (mins)	m/z	Adduct	Metabolite name	MS DIAL Match Score	MZmine Similarity score	GNPS MQ Score
1	4.58	409.1332	$[M+HCOO]^-$	Harpagide	x	0.922	x
2	5.60	137.0247	$[M-H]^-$	Protocatechuic aldehyde	1.676	x	x
3	6.41	337.0915	$[M-H]^-$	p-Coumaroylquinic acid	x	0.895	x
4	6.69	371.0933	$[M-H]^-$	6-(3-benzoyloxy-2-hydroxypropoxy)-3,4,5-trihydroxyoxane-2-carboxylic acid	1.722	x	x
5	8.52	137.0244	$[M-H]^-$	Salicylic acid (2-hydroxybenzoic acid)	1.872	x	x
5	8.60	539.1741	[M+HCOO]-	Harpagoside	x	0.915	x
6	8.67	495.2542	$[M-H]^-$	Leukotriene D4 (LTD4)	1.763	x	x
7	8.93	539.1721	$[M+HCOO]^-$	Harpagoside	x	0.943	x
7	8.98	471.1277	$[M-H]^-$	[7-acetyloxy-6-hydroxy-2-methyl-10-oxo-2,3,6,7,8,9-hexahydrooxecin-3-yl] but-2-enoate	1.720	0.850	x
8	9.16	285.0392	$[M-H]^-$	Luteolin	1.662	x	x
9	9.82	327.2156	$[M-H]^-$	9,12,13-trihydroxyoctadeca-10,15-dienoic acid	1.600	0.850	0.896
9	9.82	395.2030	$[M+Na-2H]^-$	Tsangane L 3-glucoside	x	x	0.725
10	9.99	269.0459	$[M-H]^-$	Apigenin	1.784	x	x
11	10.30	329.2317	$[M-H]^-$	5,8,11-trihydroxyoctadec-9-enoic acid	1.762	0.903	x
11	10.30	329.2317	$[M-H]^-$	9,12,13-trihydroxyoctadec-10-enoic acid	x	x	0.919
12	12.12	293.1751	$[M+CH_3COO]^-$	2-[8,8a-dimethyl-2,3,5,6,7,8-hexahydro-1H-naphthalen-2-yl]prop-2-enoic acid	1.771	x	x
13	13.04	721.3617	$[M+HCOO]^-$	Digalactosyl mono-α-linolenoyl glycerol (DGMG 18:3)	1.865	0.734	0.786
14	14.42	559.3079	$[M+HCOO]^-$	9,12,15-Octadecatrienoic acid, 3-(hexopyranosyloxy)-2-hydroxypropyl ester	x	0.981	0.971
15	14.84	295.2253	$[M-H]^-$	9-hydroxy-10,12-octadecadienoic acid	1.635	x	x
16	15.17	265.1460	$[M-H]^-$	Zinniol	x	0.755	x
17	15.32	297.1515	$[M-H]^-$	Decylbenzenesulfonic acid	x	0.849	x
18	15.58	564.3283	[M+HCOO]-	LPC 18:2	1.765	x	x
19	15.93	571.2853	$[M-H]^-$	1-Hexadecanoyl-sn-glycero-3-phospho-(1'-myo-inositol)	x	0.920	x
20	16.06	311.1660	$[M-H]^-$	Pyrenophorol	x	x	0.810
21	16.88	540.3258	$[M+HCOO]^-$	LPC 16:0	1.482	x	x
22	17.52	325.1817	$[M-H]^-$	Dodecylbenzenesulfonic acid	x	0.920	x
23	17.52	325.1820	$[M-H]^-$	Hydroquinidine	x	x	0.884
24	18.90	339.1971	$[M-H]^-$	Canrenone	1.591	0.914	0.924

Harpagide was detected in negative mode as the formate adduct $[M+HCOO]^-$ at m/z 409.1332 (RT 4.58 min; Fig.-4) and in positive mode as $[M+Na]^+$ at *m/z* 387.1246. Its MS/MS spectrum showed typical iridoid glycoside fragmentation with neutral losses corresponding to sugar cleavage and aglycone

formation. Cinnamate was detected in positive mode as $[M+H]^+$ at *m/z* 149.0588. Chromatographically, harpagide eluted at RT 4.58 min, whereas cinnamate co-eluted with harpagoside, indicating that harpagide is an independent metabolite while cinnamate likely originates from in-source fragmentation of harpagoside. LC-MS/MS profiling of *P. cornutus* also revealed oxylipins, phenolic compounds, and lipid-related metabolites. A distinct oxylipin cluster included *m/z* 327.2156 (RT 9.82 min), annotated as 9,12,13-trihydroxyoctadeca-10,15-dienoic acid based on spectral matching and SIRIUS prediction (Fig.-4B), along with related fatty acid derivatives such as α-linolenic acid. Flavonoids (luteolin, apigenin) and simple phenolics were also detected. In positive mode, a lipid cluster was annotated as monoacylglycerols (MAG 16:0 and MAG 18:0) supported by MS/MS fragmentation and in silico prediction, together with LPC species.

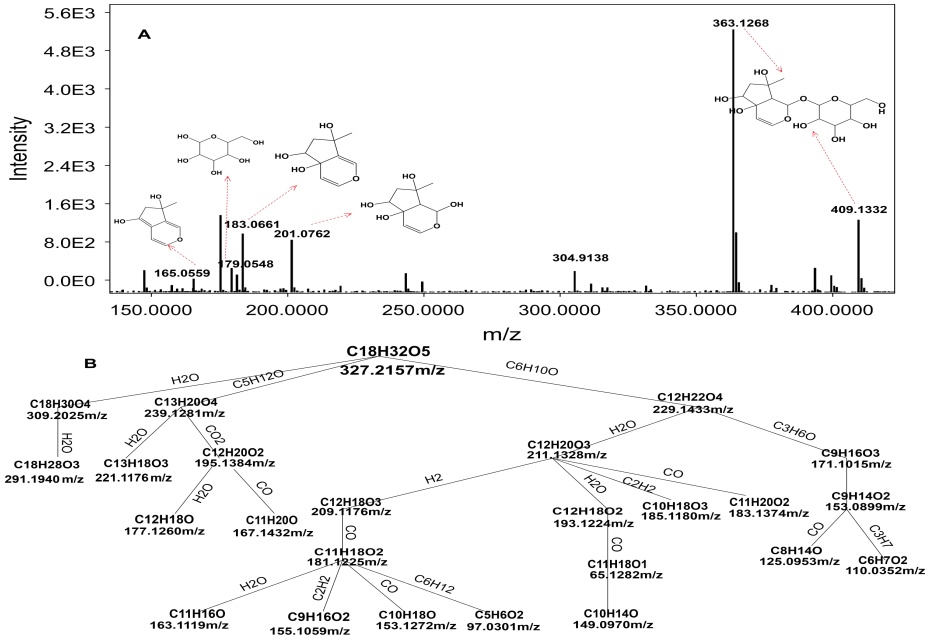

Fig.-4: Negative ESI-CID MS/MS Spectrum of the Precursor Ion at *m/z* 409.1332 ($[M+HCOO]^-$). B. SIRIUS-Derived Fragmentation Tree of the Precursor Ion at *m/z* 327.2156

At the "most specific class" level in ClassyFire, subclass predictions from CANOPUS in SIRIUS showed that negative ion mode provided broader structural coverage with 101 subclasses (Fig.-5A), mainly including carboxylic acids such as amino acids and peptides, fatty acyls like linoleic and long-chain fatty acids, and organooxygen compounds including O-glycosyls, hexoses, and O-glucuronides; prenol lipids were also diverse, largely consisting of diterpenoids and iridoid glycosides, which contributed to higher entropy. In contrast, the positive ion mode was more condensed with 65 subclasses and enriched in terpenoid-related compounds, where prenol lipids were dominated by diterpenoids, triterpenes, iridoid glycosides, xanthophylls, and limonoids, alongside benzoic and salicylic acid derivatives and mono- and diacylglycerols(Fig.-5B). The present study expands the phytochemical characterisation of *P. cornutus* beyond previous GC-MS-based profiling, which relied mainly on low-resolution library matching without MS/MS-resolved structural interpretation.[8] By integrating LC-HRMS/MS with MZmine, MS-DIAL, GNPS, SIRIUS, and manual de novo fragmentation analysis, this work enabled more confident annotation of structurally diverse and polar metabolites, particularly iridoid glycosides such as harpagoside and harpagide. The combined interpretation of positive and negative ionisation modes further improved annotation coherence across related ion species.

In vitro Bioactivities of the P. *cornutus* Extract

Within chemical classes isolated, the dominant subclasses included iridoid glycosides, hydroxylated diterpenoids, oxylipins, and monoacylglycerols, together with phenolic-related metabolites. This profile suggests the coexistence of terpenoid metabolites associated with inflammatory pathway modulation and

redox-active compounds capable of radical scavenging. Accordingly, bioactivity assays were performed to evaluate nitric oxide inhibition. Compared with the previous study, which evaluated antioxidant activity only by DPPH assay, the present work also broadened the biological characterisation through complementary $ABTS^{\bullet+}$ and FRAP assays, providing a more comprehensive assessment of redox-related bioactivity.

Inhibition of Nitric Oxide (NO) Production

The inhibitory effect of *P. cornutus* extract on nitric oxide (NO) production in LPS-stimulated RAW 264.7 macrophages is summarised in Table-2. The extract exhibited a concentration-dependent reduction of NO production, with nonlinear regression analysis yielding an IC_{50} value of 19.27 ± 1.76 µg/mL. Under identical experimental conditions, dexamethasone, as a positive control, showed stronger inhibitory activity of 12.55 ± 1.32 µM (4.93 ± 0.52 µg/mL**)**. Cell viability remained above 95% across all tested concentrations, indicating that the observed inhibition was not associated with cytotoxic effects. The low standard deviations and consistent dose-response trend further support the reliability of the estimated IC_{50}.

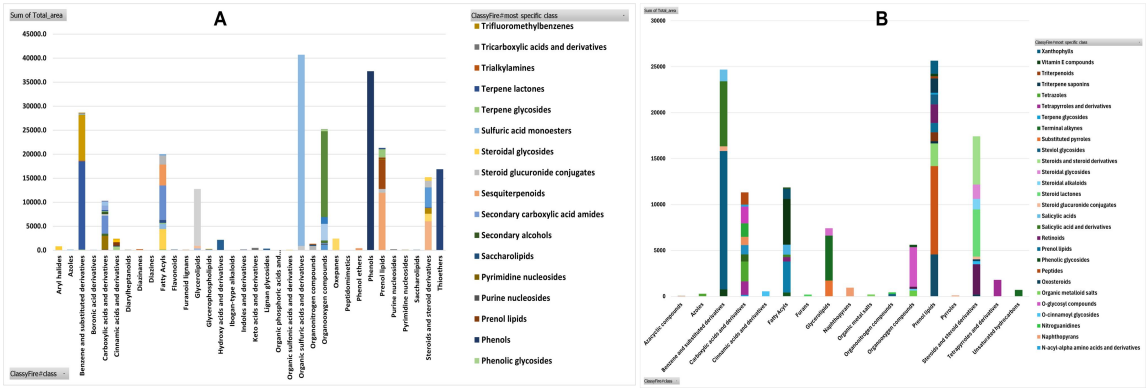

Fig.-5: Distribution of ClassyFire "Most Specific Classes" in A. Negative Ion Mode and B. Positive Ion Mode. Each Stacked Bar Represents One Classyfire Chemical Class, and the Colored Segments Correspond to Its Constituent Most Specific Classes. Bar Height Indicates the Summed Peak Area

Table-2: Inhibitory Effect of *P. cornutus* and Dexamethasone on NO Production. Results for NO Inhibition are Given as Per cent Values Relative to the LPS-Treated Control

Concentration (µM)	Dexamethasone				Concentration (µg/mL)	*P. cornutus*			
	% NO inhibition		% viable cells			% NO inhibition		% viable cells	
	Mean	SD	Mean	SD		Mean	SD	Mean	SD
100	87.8	100	95.85	1.41	100	99.66	1.96	95.26	1.32
20	54.02	20	98.81	1.22	20	50.17	1.67	96.93	1.42
4	42.98	4			4	29.83	1.84		
0.8	31.62	0.8			0.8	18.56	1.48		

$ABTS^{\bullet+}$ Radical Scavenging Activity

The ABTS assay results (Fig.-6) showed that the antioxidant capacity of *P. cornutus* extract ranged from approximately 80-90 to 213-230 mg Trolox/g extract across the tested concentration range. A gradual decrease in TEAC values with increasing extract concentration was consistently observed, while all absorbance values remained within the linear range of the Trolox calibration curves. This trend likely reflects stoichiometric and kinetic effects of the ABTS system when applied to a multicomponent extract rather than calibration artifacts. Overall, the results indicate a clear radical scavenging activity of *P. cornutus* extract consistent with the presence of multiple antioxidant constituents.

Ferric Reducing Antioxidant Power (FRAP)

Ferric reducing capacity of the *P. cornutus* extract was evaluated over 150 min at concentrations of 150-400 ppm (Fig.-7). Ferric equivalence increased progressively during the first 60-90 min and then approached a plateau, indicating a time-dependent but kinetically limited reduction process. The response

was inversely related to concentration, with 150 ppm showing higher ferric equivalence (≈11.2-15.3 mg Fe^{2+}/g extract) than 400 ppm (≈8.9-10.7 mg Fe^{2+}/g extract).

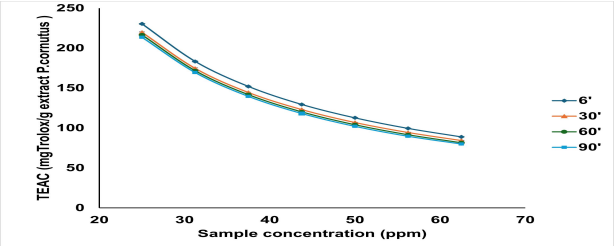

Fig.-6: TEAC Values of the *P. cornutus* Extract at different Concentrations (25-62.5 ppm) Measured at 6, 30, 60, and 90 min

This non-linear concentration-response behaviour likely reflects matrix effects or partial saturation of the reaction system at higher doses. Overall, the extract exhibited measurable ferric reducing power with both concentration- and time-dependent characteristics.

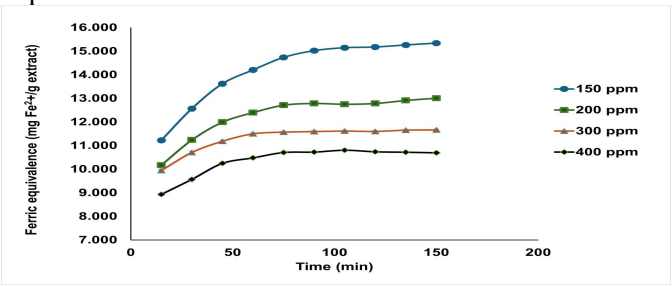

Fig.-7: Ferric Reducing Capacity of the *P. cornutus* Extract at 150-400 ppm over 150 min, Expressed as mg Fe^{2+}/g Extract

CONCLUSION

Integrated analysis of positive and negative UPLC-HRMS/MS revealed that the metabolite profile of *P. cornutus* is dominated by iridoid glycosides (harpagoside and harpagide), hydroxylated diterpenoids, oxylipins, monoacylglycerols, and minor phenolic compounds. Bioactivity assays further demonstrated concentration-dependent nitric oxide inhibition (IC_{50} = 19.27 ± 1.76 µg/mL) without cytotoxicity, together with measurable antioxidant activity in both $ABTS^{\cdot+}$ and FRAP assays. The observed NO inhibitory activity, together with the absence of detectable cytotoxicity, suggests that *P. cornutus* may represent a promising source of bioactive metabolites relevant to inflammatory pathway modulation.

ACKNOWLEDGEMENTS

The authors thank the Faculty of Chemical Engineering, IUH, for providing instruments and support for bioactivity testing in this study.

CONFLICT OF INTERESTS

The authors have no conflict of interest to declare.

AUTHOR CONTRIBUTIONS

The present work is related to *SDG-3: Good Health and Well-Being*. All the authors contributed significantly to this manuscript, participated in reviewing/editing and approved the final draft for publication. The research profile of the authors can be verified from their ORCID ids, given below:

Thi Thanh Nha Tran https://orcid.org/0000-0003-4792-6540
Thi Phuong Nhung Tran https://orcid.org/0000-0001-5733-8545

Cite this article as: T. T. Nha Tran and T. P. Nhung Tran, *Rasayan J. Chem.*, 19(3), 1396-1403(2026), https://doi.org/10.31788/RJC.2026.1939825

REFERENCES

1. K. Dührkop, M. Fleischauer, M. Ludwig, A. Aksenov, A. Melnik, M. Meusel, P. Dorrestein, J. Rousu, S. B. SIRIUS, *Nature Methods,* **16**, 299(2019), https://doi.org/10.1038/s41592-019-0344-8.
2. M. Wang, J. J. Carver, V. V. Phelan, L. M. Sanchez, N. Garg, Y. Peng, D. D. Nguyen, J. Watrous, C. A. Kapono, T. Luzzatto-Knaan, *Nature Biotechnology,* **34**, 828(2016), https://doi.org/10.1038/nbt.3597.
3. T. Pluskal, S. Castillo, A. Villar-Briones, M. Orešič, *BMC Bioinformatics,* **11**, 395(2010), https://doi.org/10.1186/1471-2105-11-395.
4. R. Schmid, S. Heuckeroth, A. Korf, A. Smirnov, O. Myers, T. S. Dyrlund, R. Bushuiev, K. J. Murray, N. Hoffmann, M. Lu, *Nature Biotechnology,* **41**, 447(2023), https://doi.org/10.1038/s41587-023-01690-2.
5. H. Tsugawa, K. Ikeda, M. Takahashi, A. Satoh, Y. Mori, H. Uchino, N. Okahashi, Y. Yamada, I. Tada, P. Bonini, *Nature Biotechnology,* **38**, 1159(2020), https://doi.org/10.1038/s41587-020-0531-2.
6. G. A. Vitale, C. Geibel, V. Minda, M. Wang, A. T. Aron, D. Petras, *Natural Product Reports,* **41**, 885(2024), https://doi.org/10.1039/D3NP00050H.
7. S. Heuckeroth, T. Damiani, A. Smirnov, O. Mokshyna, C. Brungs, A. Korf, J. D. Smith, P. Stincone, N. Dreolin, L.-F. Nothias, *Nature Protocols,* **19**, 2597(2024), https://doi.org/10.1038/s41596-024-00996-y.
8. D. H. Truong, T. N. Luu, N. T. A. Huynh, N. H. Ngo, V. S. Le, Q. H. Nguyen, T. T. Le, *Plant Science Today,* **10**, 266(2023), https://doi.org/10.14719/pst.2063.
9. Q. Wu, R. F. Ma, H. Zhang, *Phytochemistry*, **244**, Article 114757(2025), https://doi.org/10.1016/j.phytochem.2025.114757
10. S. Kheawchaum, C. Mahidol, S. Thongnest, J. Boonsombat, P. Batsomboon, S. Sitthimonchai, S. Ruchirawat, H. Prawat, *Phytochemistry,* **201**, 113261(2022), https://doi.org/10.1016/j.phytochem.2022.113261.
11. K. V. Chanu, L. G. Devi, S. K. Srivastava, M. Kataria, D. Thakuria, S. Kumar, *Indian Journal of Experimental Biology,* **59**, 153(2021), https://doi.org/10.56042/ijeb.v59i03.46965.
12. X. H. Yuan, B. G. Li, X. Y. Zhang, H. Y. Qi, M. Zhou, G. L. Zhang, *Journal of Natural Products,* **68**, 86(2005), https://doi.org/10.1021/np0497999.
13. H. C. Xi, Y. M. Shui, X. D. Ma, J. Y. Shen, H. Lai, H. B. Mo, W. G. Wang, *Nordic Journal of Botany,* **2025**, e04585(2025), https://doi.org/10.1002/njb.04585.
14. A. Mukherjee, M. Chaliha, S. Das, *Bangladesh Journal of Pharmacology,* **4**, 147(2009), https://doi.org/10.3329/bjp.v4i2.3808.
15. S. Cheenpracha, E. J. Park, B. Rostama, J. M. Pezzuto, L. C. Chang, *Marine Drugs,* **8**, 429(2010), https://doi.org/10.3390/md8030429.
16. P. J. Tsai, T. H. Tsai, C. H. Yu, S. C. Ho, *Food Chemistry,* **103**, 181(2007), https://doi.org/10.1016/j.foodchem.2006.08.013.
17. N. R. Bernardes, M. Heggdorne-Araújo, I. F. Borges, F. M. Almeida, E. P. Amaral, E. B. Lasunskaia, M. F. Muzitano, D. B. Oliveira, *Revista Brasileira de Farmacognosia,* **24**, 644(2014), https://doi.org/10.1016/j.bjp.2014.10.012.
18. M. B. Arnao, A. Cano, M. Acosta, *Food Chemistry,* **73**, 239(2001), https://doi.org/10.1016/S0308-8146(00)00324-1.
19. R. Re, N. Pellegrini, A. Proteggente, A. Pannala, M. Yang, C. Rice-Evans, *Free Radical Biology and Medicine,* **26**, 1231(1999), https://doi.org/10.1016/S0891-5849(98)00315-3.
20. I. F. Benzie, J. J. Strain, *Analytical Biochemistry,* **239**, 70(1996), https://doi.org/10.1006/abio.1996.0292.
21. M.-X. Li, X.-R. He, R. Tao, X. Cao, *The American Journal of Chinese Medicine,* **42**, 1071(2014), https://doi.org/10.1142/S0192415X14500670.

[RJC-9825/2026]